Journal Pre-proof

Spectral Spherical Harmonics Discrete Ordinate Method

Adrian Doicu, Michael I. Mishchenko, Dmitry S. Efremenko, Thomas Trautmann

PII: S0022-4073(20)30758-5
DOI: https://doi.org/10.1016/j.jqsrt.2020.107386
Reference: JQSRT 107386

To appear in: *Journal of Quantitative Spectroscopy & Radiative Transfer*

Received date: 2 September 2020
Revised date: 12 October 2020
Accepted date: 12 October 2020

Please cite this article as: Adrian Doicu, Michael I. Mishchenko, Dmitry S. Efremenko, Thomas Trautmann, Spectral Spherical Harmonics Discrete Ordinate Method, *Journal of Quantitative Spectroscopy & Radiative Transfer* (2020), doi: https://doi.org/10.1016/j.jqsrt.2020.107386

1. Radiative transfer in inhomogeneous three-dimensional media.
2. Spectral method for solving the radiative transfer equation.
3. Spherical harmonics discrete ordinate method.

Spectral Spherical Harmonics Discrete Ordinate Method

Adrian Doicu[a], Michael I. Mishchenko[b†], Dmitry S. Efremenko[a] and Thomas Trautmann[a]

[a] *Deutsches Zentrum für Luft- und Raumfahrt (DLR), Institut für Methodik der Fernerkundung (IMF), Oberpfaffenhofen 82234, Germany*

[b] *NASA Goddard Institute for Space Studies, 2880 Broadway, New York, NY 10025, USA*

Abstract

A new method for modeling the radiative transfer in inhomogeneous three-dimensional media illuminated by a Gaussian beam is described. This approach, called the Spectral Spherical Harmonics Discrete Ordinate Method (SSHDOM), uses the Fourier expansion method to transform the three-dimensional radiative transfer into an one-dimensional equation in the spectral domain, and the Spherical Harmonics Discrete Ordinate Method (SHDOM) for its solution. Specifically, (i) the source function is represented in the spectral domain through a spherical harmonic expansion, (ii) the spectral one-dimensional radiative transfer equation is integrated along discrete ordinates through a spatial grid, and (iii) the solution method is based on the Picard iteration. Both SSHDOM and SHDOM algorithms are implemented in a common computer code.

Keywords: SHDOM, Gaussian beam, three-dimensional radiative trasnfer models

1. Introduction

The scattering by a discrete random medium illuminated by a Gaussian beam is relevant to studies of spatially narrow optical beams propagating in scattering media such as fog, clouds, and biological tissue. In Ref. [1] we derived the radiative transfer equation for such media starting from the Maxwell equations, and showed that the traditional radiative transfer equation relies on the assumption of a weakly focused Gaussian beam. Application of the Fourier transform to the radiative transfer equation with respect to the horizontal variables leads to an one-dimensional radiative transfer equation in the Fourier or the spectral domain. In Ref. [2] we considered the case of a homogeneous slab, and solved the spectral one-dimensional equation by means of the discrete ordinate method with matrix exponential. A similar approach based on the discrete ordinate method in conjunction with an eigenvalue solution method was used by Kobayashi [3].

However, for an inhomogeneous medium illuminated by a Gaussian beam, the application of discrete ordinate method with matrix exponential is inefficient. The reason is that by assembling the layers equations (derived by the matrix exponential method) into a global system of equations, we are faced with the computation of the eigenvectors and eigenvalues of a large-sized matrix. Therefore, apart from the fact that the computational process is very time consuming, an increase in the size of a matrix leads to a less accurate result in the calculation for the eigenvalues. More efficient seems to be spectral methods based on the interaction principle. Along this line, we mention that Diner and Martonchik [4], and in an independent work, Stephens [5], used the interaction principle to derive adding and doubling relations for computing the reflection and transmission matrices of an inhomogeneous atmosphere bounded below by a surface with general reflection properties. In this approach, the atmosphere is divided into layers that are approximately vertically uniform, the reflection and transmission matrices are calculated via doubling for each layer, and then by repeated use of the adding formulas, the global radiative response of the entire atmosphere is determined. Latter on, Gabriel et. al [6] developed the Fourier–Riccati method relying

[†] This paper is dedicated to the memory of the late Michael I. Mishchenko, a beautiful mind and a brilliant scientist.

on a differential formulation for the reflection and transmission matrices. In this approach, the two-point boundary value problem is transformed into an initial value problem, and the resulting system of nonlinear matrix differential equations (in which the matrix equation for the reflection matrix is the Riccati matrix differential equation) is solved by using a fourth-order Runge–Kutta solver.

In this paper we present a spectral method for modeling the radiative transfer in inhomogeneous three-dimensional media. The approach is essentially based on the discrete ordinate method, but instead of assembling the layer equations into a large-sized matrix, we use a sort of successive order of scattering solution method. Actually, we solve the spectral one-dimensional equation by means of the Spherical Harmonics Discrete Ordinate Method (SHDOM) developed by Evans [7]. The resulting method called Spectral Spherical Harmonics Discrete Ordinate Method (SSHDOM) is very similar to SHDOM. For this reason, we implement SSHDOM in the SHDOM computer code [8]. To emphasize the similarities between the two methods, we summarize the SHDOM algorithm in Section 2, and then describe the SSHDOM algorithm in Section 3. Some numerical results are illustrated in Section 4.

2. Spherical Harmonics Discrete Ordinate Method

In SHDOM, the radiative transfer equation is solved iteratively by using the spherical harmonic and the discrete ordinate representations of the radiative transfer fields. In this section, after formulating the radiative transfer equation for an inhomogeneous three-dimensional medium illuminated by a Gaussian beam, we summarize some algorithm details of SHDOM.

2.1. Radiative transfer equation

The radiative transfer equation for the diffuse radiance is

$$\frac{\partial I}{\partial s}(\mathbf{r},\widehat{\mathbf{\Omega}}) = -\sigma_{\rm ext}(\mathbf{r})I(\mathbf{r},\widehat{\mathbf{\Omega}}) + J(\mathbf{r},\widehat{\mathbf{\Omega}};I), \tag{1}$$

where $I(\mathbf{r},\widehat{\mathbf{\Omega}})$ is the radiance in the direction $\widehat{\mathbf{\Omega}}$ at $\mathbf{r}$, $\sigma_{\rm ext}(\mathbf{r})$ the extinction coefficient, and $J(\mathbf{r},\widehat{\mathbf{\Omega}};I)$ the source function. The domain of analysis is chosen as a rectangular prism with the quadratic basis

$$D_{\rm xy} = \{(x,y) \mid 0 \le x \le L,\ \ 0 \le y \le L\}, \tag{2}$$

and height H.

The incident radiation is a Gaussian beam propagating in the downward direction ($\theta_0 > \pi/2$, $\varphi_0 = 0$)

$$\widehat{\mathbf{\Omega}}_0 = \sin\theta_0\widehat{\mathbf{x}} + \cos\theta_0\widehat{\mathbf{z}}, \tag{3}$$

while the center of the Guassian beam is located at the point $(L/2, L/2, H)$ of a Cartesian coordinate system (Fig. 1). The radiance field associated to the Gaussian beam is given by

$$I_0(x,y,z) = \exp\Big\{-\Big[\frac{x-x_0(z)}{s_{\rm x}}\Big]^2 - \Big(\frac{y-y_0}{s_{\rm y}}\Big)^2\Big\}\mathrm{e}^{-\tau_0(\mathbf{r})}, \tag{4}$$

where

$$x_0(z) = \frac{L}{2} + (H-z)\tan(\pi-\theta_0),\ \ y_0 = \frac{L}{2}, \tag{5}$$

$s_{\rm x}$ and $s_{\rm y}$ are the standard deviations of the Gaussian beam profile, and $\tau_0(\mathbf{r})$ is the optical depth along the incident direction.

The boundary conditions are chosen as follows. At the vertical boundaries, we assume periodic boundary conditions, at $z = H$ we impose that the downward diffuse intensity vanishes ($\mu = \cos\theta$),

$$I(x,y,H,-\mu,\varphi) = 0,\ \ \mu > 0, \tag{6}$$

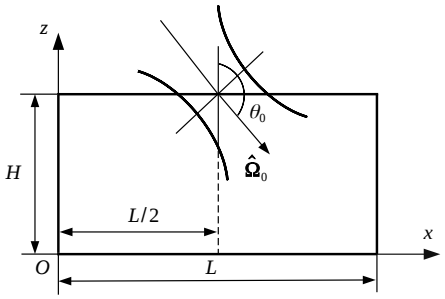

Figure 1: Domain of analysis.

and finally, at $z = 0$, we assume the Lambertian boundary condition

$$I(x,y,0,\mu,\varphi) = \frac{A(x,y)}{\pi}\mu_0 I_0(x,y,0) + \frac{A(x,y)}{\pi}\int_0^{2\pi}\int_0^1 I(x,y,0,-\mu',\varphi')\mu'\,\mathrm{d}\mu'\mathrm{d}\varphi',\ \ \mu>0, \tag{7}$$

where $A(x,y)$ is the surface albedo.

Neglecting the thermal contribution, the source function is given by

$$J(\mathbf{r},\widehat{\mathbf{\Omega}};I) = \frac{\sigma_{\mathrm{sct}}(\mathbf{r})}{4\pi}P(\mathbf{r},\widehat{\mathbf{\Omega}},\widehat{\mathbf{\Omega}}_0)I_0(\mathbf{r}) + \frac{\sigma_{\mathrm{sct}}(\mathbf{r})}{4\pi}\int P(\mathbf{r},\widehat{\mathbf{\Omega}},\widehat{\mathbf{\Omega}}')I(\mathbf{r},\widehat{\mathbf{\Omega}}')\,\mathrm{d}^2\widehat{\mathbf{\Omega}}', \tag{8}$$

where $\sigma_{\mathrm{sct}}(\mathbf{r})$ is the scattering coefficient, $P(\mathbf{r},\widehat{\mathbf{\Omega}},\widehat{\mathbf{\Omega}}')$ the scattering phase function, and $\widehat{\mathbf{\Omega}}$ and $\widehat{\mathbf{\Omega}}'$ the scattered and incident directions, respectively.

2.2. Algorithm details

As already mentioned, SHDOM uses both spherical harmonics and discrete ordinates to represent the radiance field during different parts of the solution algorithm. The spherical harmonics are employed for computing the source function including the scattering integral, while the discrete ordinates are used to integrate the radiative transfer equation spatially. Specifically, the radiative transfer equation is solved iteratively, whereby each iteration consists of four steps: (i) the transformation of the source function from spherical harmonics to discrete ordinates, (ii) the integration of the source function along discrete ordinate directions to compute the radiance field, (iii) the transformation of the discrete ordinate radiances to spherical harmonics, and (iv) the calculation of the source function from the radiance in the spherical harmonic space.

Some algorithm details are give below.

1. The radiance and source function are expanded in terms of the spherical harmonics $Y_l^m(\widehat{\mathbf{\Omega}})$. These real-valuated functions, defined by

$$Y_l^m(\theta,\varphi) = \begin{cases} \sqrt{\frac{2l+1}{2\pi}\frac{(l-|m|)!}{(l+|m|)!}}P_l^{|m|}(\cos\theta)\sin(|m|\varphi), & m<0,\\ \sqrt{\frac{2l+1}{4\pi}}P_l(\cos\theta), & m=0,\\ \sqrt{\frac{2l+1}{2\pi}\frac{(l-|m|)!}{(l+|m|)!}}P_l^{|m|}(\cos\theta)\cos(m\varphi), & m>0, \end{cases} \tag{9}$$

and orthonormal, i.e.,

$$\int_0^{2\pi}\int_0^{\pi} Y_l^m(\theta,\varphi)Y_{l'}^{m'}(\theta,\varphi)\,\sin\theta \mathrm{d}\theta\mathrm{d}\varphi = \delta_{mm'}\delta_{ll'}, \tag{10}$$

where $P_l^{|m|}$ are the associated Legendre functions and $\delta_{ll'}$ is the Kronecker delta. The expansions of the radiative transfer fields in terms of spherical harmonics read as

$$I(\mathbf{r},\widehat{\mathbf{\Omega}}) = \sum_{lm} I_{lm}(\mathbf{r})Y_l^m(\widehat{\mathbf{\Omega}}), \tag{11}$$

$$I_{lm}(\mathbf{r}) = \int_\Omega I(\mathbf{r},\widehat{\mathbf{\Omega}})Y_l^m(\widehat{\mathbf{\Omega}})\,\mathrm{d}^2\widehat{\mathbf{\Omega}}, \tag{12}$$

and

$$J(\mathbf{r},\widehat{\mathbf{\Omega}};I) = \sum_{lm} J_{lm}(\mathbf{r};I)Y_l^m(\widehat{\mathbf{\Omega}}), \tag{13}$$

$$J_{lm}(\mathbf{r};I) = \int_\Omega J(\mathbf{r},\widehat{\mathbf{\Omega}};I)Y_l^m(\widehat{\mathbf{\Omega}})\,\mathrm{d}^2\widehat{\mathbf{\Omega}} \tag{14}$$

with Ω being the unit sphere.

2. In the spherical harmonic space, the source function is computed as

$$J_{lm}(\mathbf{r};I) = \eta_l(\mathbf{r})I_{lm}(\mathbf{r}) + \eta_{0l}(\mathbf{r})Y_l^m(\widehat{\mathbf{\Omega}}_0), \tag{15}$$

where

$$\eta_l(\mathbf{r}) = \frac{\sigma_{\mathrm{sct}}(\mathbf{r})}{2l+1}\chi_l(\mathbf{r}), \tag{16}$$

$$\eta_{0l}(\mathbf{r}) = \frac{\sigma_{\mathrm{sct}}(\mathbf{r})}{2l+1}\chi_l(\mathbf{r})I_0(\mathbf{r}), \tag{17}$$

and $\chi_l(\mathbf{r})$ are the expansion coefficients of the phase function in terms of the Legendre polynomials $P_l(\cos\Theta)$, that is,

$$P(\mathbf{r},\widehat{\mathbf{\Omega}},\widehat{\mathbf{\Omega}}') = P(\mathbf{r},\widehat{\mathbf{\Omega}}\cdot\widehat{\mathbf{\Omega}}') = P(\mathbf{r},\cos\Theta) = \sum_l \chi_l(\mathbf{r})P_l(\cos\Theta). \tag{18}$$

From Eq. (15) it is clear that it is faster to compute the source function using spherical harmonics than discrete ordinates.

3. The spherical harmonic expansions are truncated at some order. More precisely, the infinite sum is approximated by the finite sum $\sum_{lm} \approx \sum_{m=-M}^{M}\sum_{l=|m|}^{L}$, that is, the degree l is assumed to range between 0 and L, and the Fourier azimuthal model m from $-M$ to M. Note that if $M = L$, the spherical harmonic truncation is triangular, which has equal angular resolution in all directions. The number of spherical harmonic terms is

$$N_{lm} = (2M+1)(L+1) - M(M+1),$$

so that in the case $M = L$, we have $N_{lm} = (L+1)^2$. For two-dimensional radiative transfer, only cosine azimuth modes are needed, in which case, $N_{lm} = (L+1)(L/2+1)$.

4. During the computational process, the method transforms between the discrete ordinate and spherical harmonic representations. The set of discrete ordinates consists of a set of Gauss-Legendre quadrature points and weights $\{\mu_i, w_{\mu i}\}_{i=1}^{N_\mu}$ in the interval $[-1,1]$, and a set of equidistant quadrature points and weights $\{\varphi_j, w_{\varphi j}\}_{j=1}^{N_\varphi}$ in the interval $[0,2\pi]$. Actually, the discrete ordinate set is reduced by taking fewer azimuth angles at larger $|\mu|$ (near the poles), so that N_φ depends on μ_i. In this case, for each μ_i, we take $\varphi_{ij} = 2\pi(j-1)/N_{\varphi i}$ and $w_{\varphi ij} = 2\pi/N_{\varphi i}$ for $j = 1, ..., N_{\varphi i}$, where $N_{\varphi i} = [0.9 + N_\varphi\sqrt{1-\mu_i^2}]$ and $[x]$ means the integer part of x.

5. The radiance and source functions are characterized, respectively,
   (a) in the Spherical Harmonic (SH) space by the expansion coefficients $I_{lm}(\mathbf{r})$ and $J_{lm}(\mathbf{r};I)$, and
   (b) in the Discrete Ordinate (DO) space by the discrete ordinate values $I(\mathbf{r},\widehat{\mathbf{\Omega}}_{ij})$ and $J(\mathbf{r},\widehat{\mathbf{\Omega}}_{ij};I)$, where $\widehat{\mathbf{\Omega}}_{ij}=(\arccos\mu_i,\varphi_j)$.
6. The solution method is a Picard iteration based on the integral form of the radiative transfer equation, that is,

$$I^{(k)}(s)=I^{(k)}(0)\mathrm{e}^{-\int_0^s\sigma_{\mathrm{ext}}(s')\,\mathrm{d}s'} + \int_0^s J(s';I^{(k-1)})\mathrm{e}^{-\int_{s'}^s\sigma_{\mathrm{ext}}(u)\,\mathrm{d}u}\,\mathrm{d}s', \tag{19}$$

   where s is a local coordinate along the discrete ordinate direction $\widehat{\mathbf{\Omega}}_{ij}$. More precisely, the process of computing the radiance field by integrating the source function along discrete ordinate directions is organized as follows:
   (a) making use on the boundary condition at $z=H$, the downward radiances are computed recursively from $z=H$ to $z=0$ by means of Eq. (19),
   (b) the upward radiances are computed at $z=0$ by using the Lambertian boundary condition (7), and
   (c) the upward radiances are computed recursively from $z=0$ to $z=H$ by means of Eq. (19).
7. To compute the path integral in Eq. (19), the variation of the extinction and source function within the grid cell are approximated from the values at the entering ($\sigma_{\mathrm{ext}}(0)$ and $J(0;I^{(k-1)})$) and exiting ($\sigma_{\mathrm{ext}}(s)$ and $J(s;I^{(k-1)})$) points. Under the assumption that these quantities, vary linearly with distance across the grid cell from $s'=0$ at the entering location to $s'=s$ at the exiting location, the computational formula is

$$I^{(k)}(s)=\mathrm{e}^{-\tau}I^{(k)}(0)+\frac{(1-\mathrm{e}^{-\tau})}{\sigma_{\mathrm{ext}}(0)+\sigma_{\mathrm{ext}}(s)} \times\Big\{J(0;I^{(k-1)})+J(s;I^{(k-1)}) +[\sigma_{\mathrm{ext}}(0)J(s;I^{(k-1)})-\sigma_{\mathrm{ext}}(s)J(0;I^{(k-1)})]T(\tau)\Big\}, \tag{20}$$

$$T(\tau)=\frac{2}{\sigma_{\mathrm{ext}}(0)+\sigma_{\mathrm{ext}}(s)}\Big(1-\frac{2}{\tau}+\frac{2\mathrm{e}^{-\tau}}{1-\mathrm{e}^{-\tau}}\Big), \tag{21}$$

$$\tau=\frac{\sigma_{\mathrm{ext}}(0)+\sigma_{\mathrm{ext}}(s)}{2}s. \tag{22}$$

8. An adaptive grid is implemented to add grid points in regions where the source function is changing more rapidly. The adaptive grid evolves from the base grid by splitting cells where more resolution is judged to be needed. The criterion for splitting cells is based on how much the source function changes across a cell. A cell may be split in half in either of the three Cartesian directions, depending on whether any of them exceed the splitting criterion.
9. For problems with the delta-M scaling method, the TMS method of Nakajima and Tanaka [9] is used to compute the source function. This method replaces the scaled, truncated Legendre phase function expansion for the singly scattered solar radiation by the full, unscaled phase function expansion.

A sketch of SHDOM is illustrated in Algorithm 1.

3. Spectral Spherical Harmonics Discrete Ordinate Method

The purpose of this section is first to formulate the radiative transfer equation in the spectral domain, and second, to provide an exhaustive description of SSHDOM and of its algorithmic implementation.

Algorithm 1 SHDOM algorithm.

• compute the extinction field $\sigma_{\text{ext}}(\mathbf{r}_n)$ and the coefficients $\eta_l(\mathbf{r}_n)$ and $\eta_{0l}(\mathbf{r}_n)$;

• initialize the SH radiances $I_{lm}^{(0)}(\mathbf{r}_n)$ with an one-dimensional radiative transfer solution, e.g., Eddington approximation or independent pixel approximation;

• use the SH radiances $I_{lm}^{(0)}(\mathbf{r}_n)$ to compute the SH source functions $J_{lm}(\mathbf{r}_n; I^{(0)})$ by means of Eq. (15);

for $k = 1, \ldots, N_{\text{iter}}$ **do** {Picard iteration}

- split cells and compute the SH source functions $J_{lm}(\cdot; I^{(k-1)})$ at the new grid points;
- transform the SH source functions $J_{lm}(\mathbf{r}_n; I^{(k-1)})$ to DO space, i.e., compute $J(\mathbf{r}_n, \widehat{\mathbf{\Omega}}_{ij}; I^{(k-1)})$ as (cf. Eq. (13))

$$J(\mathbf{r}_n, \widehat{\mathbf{\Omega}}_{ij}; I^{(k-1)}) = \sum_{m=-M}^{M} \sum_{l=|m|}^{L} J_{lm}(\mathbf{r}_n; I^{(k-1)}) Y_l^m(\widehat{\mathbf{\Omega}}_{ij});$$

- compute the DO radiances $I^{(k)}(\mathbf{r}_n, \widehat{\mathbf{\Omega}}_{ij})$ by integrating the DO source functions $J(\mathbf{r}_n, \widehat{\mathbf{\Omega}}_{ij}; I^{(k-1)})$ along the discrete ordinate direction $\widehat{\mathbf{\Omega}}_{ij}$ according to Eq. (19);
- transform the DO radiances $I^{(k)}(\mathbf{r}_n, \widehat{\mathbf{\Omega}}_{ij})$ to SH space, i.e., compute $I_{lm}^{(k)}(\mathbf{r}_n)$ as (cf. Eq. (12))

$$I_{lm}^{(k)}(\mathbf{r}_n) = \sum_{i=1}^{N_\mu} \sum_{j=1}^{N_{\varphi i}} w_{ij} I^{(k)}(\mathbf{r}_n, \widehat{\mathbf{\Omega}}_{ij}) Y_l^m(\widehat{\mathbf{\Omega}}_{ij}), \text{ where } w_{ij} = w_{\mu i} w_{\varphi ij};$$

- use the SH radiances $I_{lm}^{(k)}(\mathbf{r}_n)$ to update the SH source functions $J_{lm}(\mathbf{r}_n; I^{(k)})$ by means of Eq. (15);
- **if** ($J_{lm}(\mathbf{r}_n; I^{(k)})$ converge) **exit**

end for

• use $J_{lm}(\mathbf{r}_n; \cdot)$ to compute the radiance $I(\mathbf{r}, \widehat{\mathbf{\Omega}})$ at point $\mathbf{r}$ in direction $\widehat{\mathbf{\Omega}}$ by employing the source function integration technique;

3.1. Radiative transfer equation in the spectral domain

A method for solving the radiative transfer equation (1), endowed with the boundary conditions (6) and (7), is to consider either the Fourier transform of the diffuse intensity $I(z,\boldsymbol{\rho};\widehat{\boldsymbol{\Omega}})$ or its Fourier expansion. From a computational point of view, both methods are equivalent [2]. Here, we consider the Fourier expansion method because this approach is more suitable for practical applications.

We begin our analysis with some preliminary constructions.

1. We set

$$\mathbf{r}=\boldsymbol{\rho}+z\widehat{\mathbf{z}},\ \ \boldsymbol{\rho}=x\widehat{\mathbf{x}}+y\widehat{\mathbf{y}}, \tag{23}$$

and

$$\widehat{\boldsymbol{\Omega}}=\boldsymbol{\omega}+\cos\theta\widehat{\mathbf{z}},\ \ \boldsymbol{\omega}=\sin\theta(\cos\varphi\widehat{\mathbf{x}}+\sin\varphi\widehat{\mathbf{y}}), \tag{24}$$

and express the radiative transfer equation as

$$\mu\frac{\partial I}{\partial z}(z,\boldsymbol{\rho},\widehat{\boldsymbol{\Omega}})+\boldsymbol{\omega}\cdot\frac{\partial I}{\partial\boldsymbol{\rho}}(z,\boldsymbol{\rho},\widehat{\boldsymbol{\Omega}})=-\sigma_{\mathrm{ext}}(z,\boldsymbol{\rho})I(z,\boldsymbol{\rho},\widehat{\boldsymbol{\Omega}})+J(z,\boldsymbol{\rho},\widehat{\boldsymbol{\Omega}};I). \tag{25}$$

2. We translate the coordinate system at the point $(L/2,L/2,0)$, so that in the new coordinate system, also denoted by $Oxyz$, the quadratic basis of the rectangular prism is

$$D_{\mathrm{xy}}=\{(x,y)\mid -l\le x\le l,\ \ -l\le y\le l\}, \tag{26}$$

where $L=2l$.

The radiance field $I(z,\boldsymbol{\rho},\widehat{\boldsymbol{\Omega}})$, defined over a rectangular domain with boundaries at $\pm l$, can be extended through periodicity over the entire two-dimensional space. In this regard, we consider the Fourier expansion

$$I(z,\boldsymbol{\rho},\widehat{\boldsymbol{\Omega}})=\sum_{u=-U}^{U}\sum_{v=-U}^{U}\widehat{I}_{uv}(z,\widehat{\boldsymbol{\Omega}})\mathrm{e}^{\mathrm{j}\pi(ux+vy)/l}, \tag{27}$$

where the expansion coefficients are computed as

$$\widehat{I}_{uv}(z,\widehat{\boldsymbol{\Omega}})=\frac{1}{4l^2}\int_{-l}^{l}I(z,\boldsymbol{\rho},\widehat{\boldsymbol{\Omega}})\mathrm{e}^{-\mathrm{j}\pi(ux+vy)/l}\mathrm{d}x\mathrm{d}y. \tag{28}$$

Furthermore, considering the Fourier expansions of the source function and the extinction field, i.e.,

$$J(z,\boldsymbol{\rho},\widehat{\boldsymbol{\Omega}};I)=\sum_{u=-U}^{U}\sum_{v=-U}^{U}\widehat{J}_{uv}(z,\widehat{\boldsymbol{\Omega}};\widehat{I})\mathrm{e}^{\mathrm{j}\pi(ux+vy)/l}, \tag{29}$$

$$\widehat{J}_{uv}(z,\widehat{\boldsymbol{\Omega}};\widehat{I})=\frac{1}{4l^2}\int_{-l}^{l}J(z,\boldsymbol{\rho},\widehat{\boldsymbol{\Omega}};I)\mathrm{e}^{-\mathrm{j}\pi(ux+vy)/l}\mathrm{d}x\mathrm{d}y, \tag{30}$$

and

$$\sigma_{\mathrm{ext}}(z,\boldsymbol{\rho})=\sum_{u=-U}^{U}\sum_{v=-U}^{U}\widehat{\sigma}_{\mathrm{ext}uv}(z)\mathrm{e}^{\mathrm{j}\pi(ux+vy)/l}, \tag{31}$$

$$\widehat{\sigma}_{\mathrm{ext}uv}(z)=\frac{1}{4l^2}\int_{-l}^{l}\sigma_{\mathrm{ext}}(z,\boldsymbol{\rho})\mathrm{e}^{-\mathrm{j}\pi(ux+vy)/l}\mathrm{d}x\mathrm{d}y, \tag{32}$$

respectively, inserting Eqs. (27), (29) and (31) in Eq. (25), and making use on the convolution theorem, we obtain the following representation for the radiative transfer equation in the Fourier space:

$$\mu\frac{\mathrm{d}\widehat{I}_{uv}}{\mathrm{d}z}(z,\widehat{\mathbf{\Omega}}) = -\sum_{u'=-U}^{U}\sum_{v'=-U}^{U}\varsigma_{uv;u'v'}(z,\widehat{\mathbf{\Omega}})\widehat{I}_{u'v'}(z,\widehat{\mathbf{\Omega}}) + \widehat{J}_{uv}(z,\widehat{\mathbf{\Omega}};\widehat{I}), \tag{33}$$

where

$$\begin{aligned}\varsigma_{uv;u'v'}(z,\widehat{\mathbf{\Omega}}) &= \widehat{\sigma}_{\mathrm{ext}u-u',v-v'}(z)\\ &\quad + \mathrm{j}\frac{\pi}{l}\sqrt{1-\mu^2}(u\cos\varphi + v\sin\varphi)\delta_{uu'}\delta_{vv'}.\end{aligned} \tag{34}$$

Coming to the boundary conditions, we consider the Fourier expansions of the surface albedo

$$A(x,y) = \sum_{u=-U}^{U}\sum_{v=-U}^{U}\widehat{A}_{uv}\mathrm{e}^{\mathrm{j}\pi(ux+vy)/l}, \tag{35}$$

$$\widehat{A}_{uv} = \frac{1}{4l^2}\int_{-l}^{l}A(x,y)\mathrm{e}^{-\mathrm{j}\pi(ux+vy)/l}\mathrm{d}x\mathrm{d}y, \tag{36}$$

and of the product $R(x,y) = A(x,y)I_0(x,y,0)$,

$$R(x,y) = \sum_{u=-U}^{U}\sum_{v=-U}^{U}\widehat{R}_{uv}\mathrm{e}^{\mathrm{j}\pi(ux+vy)/l}, \tag{37}$$

$$\widehat{R}_{uv} = \frac{1}{4l^2}\int_{-l}^{l}R(x,y)\mathrm{e}^{-\mathrm{j}\pi(ux+vy)/l}\mathrm{d}x\mathrm{d}y, \tag{38}$$

to obtain

$$\widehat{I}_{uv}(H,-\mu,\varphi) = 0,\ \ \mu > 0, \tag{39}$$

at $z = H$, and

$$\begin{aligned}\widehat{I}_{uv}(0,\mu,\varphi) &= \frac{\mu_0}{\pi}\widehat{R}_{uv} + \frac{1}{\pi}\sum_{u'=-U}^{U}\sum_{v'=-U}^{U}\widehat{A}_{u-u',v-v'}\\ &\quad\times\int_0^{2\pi}\int_0^1\widehat{I}_{u'v'}(0,-\mu',\varphi')\mu'\,\mathrm{d}\mu'\mathrm{d}\varphi',\ \ \mu > 0,\end{aligned} \tag{40}$$

at $z = 0$.

Eq. (33) is analogous to the one-dimensional radiative transfer equation and together with the Fourier transformed boundary conditions (39) and (39) constitutes a two-point boundary value problem. In contrast, the radiative transfer equation (1) is a three-dimensional differential equation. Moreover, in the Fourier space, the horizontal inhomogeneities are described by the expansion coefficients $\widehat{I}_{uv}(z,\widehat{\mathbf{\Omega}})$, while in the real space and say, at the discrete points $x_p = p\Delta l$ and $y_q = q\Delta l$, the horizontal inhomogeneities are described by the radiance field $I(x_p,y_p,z,\widehat{\mathbf{\Omega}})$. The advantage of solving an one-dimensional radiative transfer equation is only apparent; the price for this conceptual simplification lies in a larger set of simultaneous integro-differential equations that governs the Fourier transformed radiances $\widehat{I}_{uv}(z,\widehat{\mathbf{\Omega}})$ for all indices $u,v = -U,\ldots,U$.

3.2. Algorithm details

Analogously to Eq. (1), the radiative transfer equation (33) is solved by using the spherical harmonics discrete ordinate method. Thus, the solution method will transform between the discrete ordinate and spherical harmonic representations. The difference is that now, these representations are considered in the Fourier space.

To explain the SSHDOM algorithm we note the following results.

1. The spherical harmonic coefficients of the radiance field $I_{lm}(z,\boldsymbol{\rho})$ can be expanded in a Fourier series; the result is

$$I_{lm}(z,\boldsymbol{\rho}) = \sum_{u=-U}^{U}\sum_{v=-U}^{U} \widehat{I}_{lm;uv}(z)\mathrm{e}^{\mathrm{j}\pi(ux+vy)/l}, \tag{41}$$

$$\widehat{I}_{lm;uv}(z) = \frac{1}{4l^2}\int_{-l}^{l} I_{lm}(z,\boldsymbol{\rho})\mathrm{e}^{-\mathrm{j}\pi(ux+vy)/l}\mathrm{d}x\mathrm{d}y, \tag{42}$$

yielding (cf. Eqs. (11), (27), and (41))

$$\widehat{I}_{uv}(z;\widehat{\boldsymbol{\Omega}}) = \sum_{lm} \widehat{I}_{lm;uv}(z)Y_l^m(\widehat{\boldsymbol{\Omega}}), \tag{43}$$

$$\widehat{I}_{lm;uv}(z) = \int_{\Omega} \widehat{I}_{uv}(z;\widehat{\boldsymbol{\Omega}})Y_l^m(\widehat{\boldsymbol{\Omega}})\,\mathrm{d}^2\widehat{\boldsymbol{\Omega}}. \tag{44}$$

2. Similarly, for the spherical harmonic coefficients of the source function $J_{lm}(z,\boldsymbol{\rho};I)$, we have

$$J_{lm}(z,\boldsymbol{\rho};I) = \sum_{u=-U}^{U}\sum_{v=-U}^{U} \widehat{J}_{lm;uv}(z;\widehat{I})\mathrm{e}^{\mathrm{j}\pi(ux+vy)/l}, \tag{45}$$

$$\widehat{J}_{lm;uv}(z;\widehat{I}) = \frac{1}{4l^2}\int_{-l}^{l} J_{lm}(z,\boldsymbol{\rho};I)\mathrm{e}^{-\mathrm{j}\pi(ux+vy)/l}\mathrm{d}x\mathrm{d}y, \tag{46}$$

yielding (cf. Eqs. (12), (29), and (45))

$$\widehat{J}_{uv}(z,\widehat{\boldsymbol{\Omega}};\widehat{I}) = \sum_{lm} \widehat{J}_{lm;uv}(z;\widehat{I})Y_l^m(\widehat{\boldsymbol{\Omega}}), \tag{47}$$

$$\widehat{J}_{lm;uv}(z;\widehat{I}) = \int_{\Omega} \widehat{J}_{uv}(z,\widehat{\boldsymbol{\Omega}};\widehat{I})Y_l^m(\widehat{\boldsymbol{\Omega}})\,\mathrm{d}^2\widehat{\boldsymbol{\Omega}}. \tag{48}$$

3. Inserting Eqs. (41) and (45) in Eq. (15), i.e.,

$$J_{lm}(\mathbf{r};I) = \eta_l(\mathbf{r})I_{lm}(\mathbf{r}) + \eta_{0l}(\mathbf{r})Y_l^m(\widehat{\boldsymbol{\Omega}}_0),$$

and using again the convolution theorem, gives

$$\begin{aligned}\widehat{J}_{lm;uv}(z;\widehat{I}) = {}& \widehat{\eta}_{0l;uv}(z)Y_l^m(\widehat{\boldsymbol{\Omega}}_0) \\ & + \sum_{u'=-U}^{U}\sum_{v'=-U}^{U} \widehat{\eta}_{l;u-u',v-v'}(z)\widehat{I}_{lm;u'v'}(z),\end{aligned} \tag{49}$$

where

$$\widehat{\eta}_{0l;uv}(z) = \frac{1}{4l^2}\int_{-l}^{l} \eta_{0l}(z,\boldsymbol{\rho})\mathrm{e}^{-\mathrm{j}\pi(ux+vy)/l}\mathrm{d}x\mathrm{d}y, \tag{50}$$

$$\widehat{\eta}_{l;uv}(z) = \frac{1}{4l^2}\int_{-l}^{l} \eta_{l}(z,\boldsymbol{\rho})\mathrm{e}^{-\mathrm{j}\pi(ux+vy)/l}\mathrm{d}x\mathrm{d}y. \tag{51}$$

4. The radiance and source functions are characterized, respectively,
   (a) in the Spherical Harmonic (SH) space by $I_{lm}(z,\boldsymbol{\rho})$ and $J_{lm}(z,\boldsymbol{\rho};I)$ (as mentioned in Section 2.2),
   (b) in the Fourier space by $\widehat{I}_{uv}(z,\widehat{\boldsymbol{\Omega}})$ and $\widehat{J}_{uv}(z,\widehat{\boldsymbol{\Omega}};I)$,
   (c) in the Spherical Harmonic Fourier (SHF) space by $\widehat{I}_{lm;uv}(z)$ and $\widehat{J}_{lm;uv}(z;\widehat{I})$, and

(d) in the Discrete Ordinate Fourier (DOF) space by the discrete ordinate values $\widehat{I}_{uv}(z, \widehat{\mathbf{\Omega}}_{ij})$ and $\widehat{J}_{uv}(z, \widehat{\mathbf{\Omega}}_{ij}; \widehat{I})$.

For radiances, Eqs. (41)–(42) give the transformations between the SH and SHF spaces, while Eqs. (43)–(44) give the transformations between the Fourier and SHF spaces. For source functions, the same transformations are provided by Eqs. (45)–(46) and (47)–(48). Note that Eq. (49), giving the expression of the SHF source function $\widehat{J}_{lm;uv}(z; \widehat{I})$ in the Fourier space, is the counterpart of Eq. (15), giving the expression of the SH source function $J_{lm}(\mathbf{r}; I)$.

5. To solve the radiative transfer equation (33), we rewrite this equation as

$$\mu \frac{\mathrm{d}\widehat{I}_{uv}}{\mathrm{d}z}(z, \widehat{\mathbf{\Omega}}) = -\varsigma_{uv;uv}(z, \widehat{\mathbf{\Omega}})\widehat{I}_{uv}(z, \widehat{\mathbf{\Omega}}) + \widehat{J}_{0uv}(z, \widehat{\mathbf{\Omega}}; \widehat{I}) + \widehat{J}_{uv}(z, \widehat{\mathbf{\Omega}}; \widehat{I}), \tag{52}$$

where

$$\widehat{J}_{0uv}(z, \widehat{\mathbf{\Omega}}; \widehat{I}) = -\sum_{u'=-U;\, u' \neq u}^{U} \sum_{v'=-U;\, v' \neq v}^{U} \widehat{\sigma}_{\mathrm{ext}u-u',v-v'}(z)\widehat{I}_{u'v'}(z, \widehat{\mathbf{\Omega}}), \tag{53}$$

and apply an iterative scheme to the integral form of Eq. (52) ($s = z/\mu_p$)

$$\widehat{I}^{(k)}_{uv}(s) = \widehat{I}^{(k)}_{uv}(0)\mathrm{e}^{-\int_0^s \varsigma_{uv;uv}(s')\,\mathrm{d}s'} + \int_0^s [\widehat{J}_{0uv}(s'; \widehat{I}^{(k-1)}) + \widehat{J}_{uv}(s'; \widehat{I}^{(k-1)})]\mathrm{e}^{-\int_{s'}^s \varsigma_{uv;uv}(u)\,\mathrm{d}u}\,\mathrm{d}s'. \tag{54}$$

A sketch of SSHDOM is illustrated in Algorithm 2. The steps written with italic fonts highlight the differences to the SHDOM algorithm.

Some comments are in order.

1. To compute the path integral (54), we use Eqs. (20)–(22) with the replacements ($s' = z'/\mu_p$)

$$J(s'; I^{(k-1)}) \to \widehat{J}_{0uv}(s'; \widehat{I}^{(k-1)}) + \widehat{J}_{uv}(s'; \widehat{I}^{(k-1)}),$$

$\sigma_{\mathrm{ext}}(0) \to \varsigma_{uv;uv}(0)$, and $\sigma_{\mathrm{ext}}(s) \to \varsigma_{uv;uv}(s)$.

2. Another iterative scheme than that given by Eq. (54) can be derived as follows. We rewrite Eq. (54) as

$$\widehat{I}^{(k)}_{uv}(s) = \widehat{I}^{(k)}_{uv}(0)\mathrm{e}^{-\int_0^s \varsigma_{uv;uv}(s')\,\mathrm{d}s'} + \int_0^s \widehat{J}_{0uv}(s'; \widehat{I}^{(k)})\mathrm{e}^{-\int_{s'}^s \varsigma_{uv;uv}(u)\,\mathrm{d}u}\,\mathrm{d}s' + \int_0^s \widehat{J}_{uv}(s'; \widehat{I}^{(k-1)})\mathrm{e}^{-\int_{s'}^s \varsigma_{uv;uv}(u)\,\mathrm{d}u}\,\mathrm{d}s', \tag{55}$$

that is, we replace $\widehat{J}_{0uv}(s'; \widehat{I}^{(k-1)})$ by $\widehat{J}_{0uv}(s'; \widehat{I}^{(k)})$. Then, using the boundary values

$$\widehat{J}_{0uv}(0; \widehat{I}^{(k)}) = -\sum_{u' \neq u} \sum_{v' \neq v} \widehat{\sigma}_{\mathrm{ext}u-u',v-v'}(0)\widehat{I}^{(k)}_{u'v'}(0), \tag{56}$$

$$\widehat{J}_{0uv}(s; \widehat{I}^{(k)}) = -\sum_{u' \neq u} \sum_{v' \neq v} \widehat{\sigma}_{\mathrm{ext}u-u',v-v'}(s)\widehat{I}^{(k)}_{u'v'}(s), \tag{57}$$

Algorithm 2 SSHDOM algorithm.

• compute the extinction field $\sigma_{\text{ext}}(\mathbf{r}_n)$ and the coefficients $\eta_l(\mathbf{r}_n)$ and $\eta_{0l}(\mathbf{r}_n)$;
• compute the Fourier transform $\widehat{\sigma}_{\text{ext}uv}(z_n)$, $\widehat{\eta}_{l;uv}(z_n)$, and $\widehat{\eta}_{0l;uv}(z_n)$ by means of Eqs. (32), (50), and (51), respectively;
• initialize the SH radiances $I^{(0)}_{lm}(\mathbf{r}_n)$ with an one-dimensional radiative transfer solution, e.g., Eddington approximation or independent pixel approximation;
• *compute the SHF radiances $\widehat{I}^{(0)}_{lm;uv}(z_n)$ by applying the Fourier transform (42) to the SH radiances $I^{(0)}_{lm}(\mathbf{r}_n)$*;
• use the SHF radiances $\widehat{I}^{(0)}_{lm;uv}(z_n)$ to compute the SHF source functions $\widehat{J}_{lm;uv}(z_n;\widehat{I}^{(0)})$ by means of Eq. (49);
for $k = 1, \ldots, N_{\text{iter}}$ **do** {Picard iteration}

- split layers and compute the SHF radiances $\widehat{I}^{(k-1)}_{lm;uv}(\cdot)$ and the SHF source functions $\widehat{J}_{lm;uv}(\cdot;\widehat{I}^{(k-1)})$ at the new level points;
- transform the SHF radiances $\widehat{I}^{(k-1)}_{lm;uv}(z_n)$ and the SHF source functions $\widehat{J}_{lm;uv}(z_n;\widehat{I}^{(k-1)})$ to DOF space, i.e., compute $\widehat{I}^{(k-1)}_{uv}(z_n,\widehat{\mathbf{\Omega}}_{ij})$ and $\widehat{J}_{uv}(z_n,\widehat{\mathbf{\Omega}}_{ij};\widehat{I}^{(k-1)})$ as (cf. Eqs. (43) and (47))

$$\widehat{I}^{(k-1)}_{uv}(z_n,\widehat{\mathbf{\Omega}}_{ij}) = \sum_{m=-M}^{M}\sum_{l=|m|}^{L} \widehat{I}^{(k-1)}_{lm;uv}(z_n)Y^m_l(\widehat{\mathbf{\Omega}}_{ij}),$$

$$\widehat{J}_{uv}(z_n,\widehat{\mathbf{\Omega}}_{ij};\widehat{I}^{(k-1)}) = \sum_{m=-M}^{M}\sum_{l=|m|}^{L} \widehat{J}_{lm;uv}(z_n;\widehat{I}^{(k-1)})Y^m_l(\widehat{\mathbf{\Omega}}_{ij});$$

- *use the DOF radiances $\widehat{I}^{(k-1)}_{uv}(z_n,\widehat{\mathbf{\Omega}}_{ij})$ to compute the DOF source functions $\widehat{J}_{0uv}(z_n,\widehat{\mathbf{\Omega}}_{ij};\widehat{I}^{(k-1)})$ by using Eq. (53)*;
- compute the DOF radiances $\widehat{I}^{(k)}_{uv}(z_n,\widehat{\mathbf{\Omega}}_{ij})$ by integrating the DOF source functions $\widehat{J}_{uv}(z_n,\widehat{\mathbf{\Omega}}_{ij};\widehat{I}^{(k-1)})$ and $\widehat{J}_{0uv}(z_n,\widehat{\mathbf{\Omega}}_{ij};\widehat{I}^{(k-1)})$ along the discrete ordinate direction $\widehat{\mathbf{\Omega}}_{ij}$ according to Eq. (54);
- transform the DOF radiances $\widehat{I}^{(k)}_{uv}(z_n,\widehat{\mathbf{\Omega}}_{ij})$ to SHF space, i.e., compute $\widehat{I}^{(k)}_{lm;uv}(z_n)$ as (cf. Eq. (44))

$$\widehat{I}^{(k)}_{lm;uv}(z_n) = \sum_{i=1}^{N_\mu}\sum_{j=1}^{N_{\varphi i}} w_{ij}\widehat{I}^{(k)}_{uv}(z_n,\widehat{\mathbf{\Omega}}_{ij})Y^m_l(\widehat{\mathbf{\Omega}}_{ij});$$

- use the SHF radiances $\widehat{I}^{(k)}_{lm;uv}(z_n)$ to update the SHF source functions $\widehat{J}_{lm;uv}(z_n;\widehat{I}^{(k)})$ by means of Eq. (49);
- **if** ($\widehat{J}_{lm;uv}(z_n;\widehat{I}^{(k)})$ converge) **exit**

end for
• *use the SHF source functions $\widehat{J}_{lm;uv}(z_n;\cdot)$ to compute the SH source functions $J_{lm}(\mathbf{r}_n;\cdot)$ according to Eq. (45)*;
• use $J_{lm}(\mathbf{r}_n;\cdot)$ to compute the radiance $I(\mathbf{r},\widehat{\mathbf{\Omega}})$ at point $\mathbf{r}$ in direction $\widehat{\mathbf{\Omega}}$ by employing the source function integration technique;

and inserting these equations in Eq. (20), we obtain

$$\begin{aligned}\widehat{I}_{uv}^{(k)}(s) = {} & \mathrm{e}^{-\tau}\widehat{I}_{uv}^{(k)}(0) - \frac{(1-\mathrm{e}^{-\tau})}{\varsigma_{uv;uv}(0)+\varsigma_{uv;uv}(s)} \\ & \times \sum_{u'\neq u}\sum_{v'\neq v}\Big\{\widehat{\sigma}_{\mathrm{ext}u-u',v-v'}(0)\widehat{I}_{u'v'}^{(k)}(0) + \widehat{\sigma}_{\mathrm{ext}u-u',v-v'}(s)\widehat{I}_{u'v'}^{(k)}(s) \\ & + [\varsigma_{uv;uv}(0)\widehat{\sigma}_{\mathrm{ext}u-u',v-v'}(s)\widehat{I}_{u'v'}^{(k)}(s) \\ & - \varsigma_{uv;uv}(s)\widehat{\sigma}_{\mathrm{ext}u-u',v-v'}(0)\widehat{I}_{u'v'}^{(k)}(0)]T(\tau)\Big\} \\ & + \frac{(1-\mathrm{e}^{-\tau})}{\varsigma_{uv;uv}(0)+\varsigma_{uv;uv}(s)}\Big\{\widehat{J}_{uv}(0;\widehat{I}^{(k-1)}) + \widehat{J}_{uv}(s;\widehat{I}^{(k-1)}) \\ & + [\varsigma_{uv;uv}(0)\widehat{J}_{uv}(s;\widehat{I}^{(k-1)}) - \varsigma_{uv;uv}(s)\widehat{J}_{uv}(0;\widehat{I}^{(k-1)})]T(\tau)\Big\}, \end{aligned} \tag{58}$$

where

$$\tau = \frac{\varsigma_{uv;uv}(0)+\varsigma_{uv;uv}(s)}{2}s. \tag{59}$$

The above equation can be written in matrix form as

$$\mathsf{A}\widehat{\mathsf{I}}^{(k)}(s) = \mathsf{A}_0\widehat{\mathsf{I}}^{(k)}(0) + \mathsf{b}, \tag{60}$$

where the elements of the column vectors $\widehat{\mathsf{I}}^{(k)}(s) \in \mathbb{R}^{(2U+1)^2}$ and $\widehat{\mathsf{I}}^{(k)}(0) \in \mathbb{R}^{(2U+1)^2}$ are $\widehat{I}_{uv}^{(k)}(s)$ and $\widehat{I}_{uv}^{(k)}(0)$, for all values of $u = -U,\ldots,U$ and $v = -U,\ldots,U$, respectively. This iterative scheme is more accurate than that given by Eq. (54) but is less efficient (the method requires the solution of the matrix equation (60)).

3. The integrals in Eqs. (32), (50), and (51) are computed by using an N-term two-dimensional discrete Fourier transform [2]. To summarize the computational algorithm, we consider the integral

$$\widehat{f}_{uv} = \frac{1}{4l^2}\int_{-l}^{l} f(x,y)\mathrm{e}^{-\mathrm{j}\pi(ux+vy)/l}\mathrm{d}x\mathrm{d}y,$$

for $u,v = -U,\ldots,U-1$, and the set of equidistant discrete points in spatial domain

$$\begin{aligned} D_{\mathrm{xy}} = \{(x_p,y_q) \mid {} & x_p = p\Delta l,\ \ y_q = q\Delta l \\ & \text{for } p,q = -U,\ldots,U-1\}, \end{aligned} \tag{61}$$

where $N = 2U = 2^s$ and $L = 2l = N\Delta l$. The steps for computing $\widehat{f}_{uv}$ are as follows:

Step 1. compute $s_{p_1q_1} = f_{p_1-U,q_1-U}\mathrm{e}^{\mathrm{j}\pi(p_1+q_1)}$
for $p_1,q_1 = 0,\ldots,N-1$, where
$f_{pq} = f(x_p,y_q)$ for $p,q = -U,\ldots,U-1$,

Step 2. compute $\widehat{s}_{u_1v_1} = \displaystyle\sum_{p_1,q_1=0}^{N-1} s_{p_1q_1}\mathrm{e}^{-\mathrm{j}\frac{2\pi}{N}(u_1p_1+v_1q_1)}$
for $u_1,v_1 = 0,\ldots,N-1$,

Step 3. compute $\widehat{f}_{uv} = \dfrac{1}{N^2}\widehat{s}_{u+U,v+U}\mathrm{e}^{\mathrm{j}\pi(u+v)}$
for $u,v = -U,\ldots,U-1$.

Note that in Step 2, the N-term two-dimensional fast Fourier transform is applied.

4. SSHDOM uses a fixed horizontal grid and an adaptive grid in the vertical direction. As in SHDOM, the criterion for splitting a layer, bounded below by z_n and above by z_{n+1}, is based on how much the SH source function changes across the layer, that is,

$$C = |\Delta\widehat{J}|(1 - \mathrm{e}^{-\tau}),$$

where τ is given by Eq. (59), and $|\Delta\widehat{J}|$ is an average difference of the SH source functions over all angles,

$$\begin{aligned}|\Delta\widehat{J}|^2 &= \frac{1}{4\pi}\int_0^{2\pi}\int_{-1}^{1} |\widehat{J}_{uv}(z_n, \widehat{\mathbf{\Omega}}; \widehat{I}^{(k-1)}) - \widehat{J}_{uv}(z_{n+1}, \widehat{\mathbf{\Omega}}; \widehat{I}^{(k-1)})|^2 \,\mathrm{d}\mu\mathrm{d}\varphi \\ &= \frac{1}{4\pi}\sum_{lm} |\widehat{J}_{lm;uv}(z_n; \widehat{I}^{(k-1)}) - \widehat{J}_{lm;uv}(z_{n+1}; \widehat{I}^{(k-1)})|^2.\end{aligned}$$

When a layer is split, $\widehat{I}^{(k-1)}_{lm;u'v'}$ and $\widehat{J}_{lm;uv}$ must be specified at the new level point $z' = (z_n + z_{n+1})/2$. For doing this, we compute

   (a) $\widehat{\sigma}_{\mathrm{ext}uv}(z')$ and $\widehat{\eta}_{l;uv}(z')$ by linear interpolation between the corresponding grid values at z_n and z_{n+1},
   (b) $I_0(\mathbf{r}')$ by using Eq. (4), where $\mathbf{r}'$ is a point having as horizontal coordinates the coordinates of a point on the base grid and z' as vertical coordinate,
   (c) the expansion coefficients $\eta_{0l}(\mathbf{r}')$ and $\widehat{\eta}_{0l;uv}(z')$ by means of Eqs. (17) and (50), respectively,
   (d) $\widehat{I}^{(k-1)}_{lm;u'v'}(z')$ by linear interpolation between the grid values at z_n and z_{n+1}, and finally,
   (e) $\widehat{J}_{lm;uv}(z'; \widehat{I}^{(k-1)})$ according to Eq. (49).

5. The pre- and post-processing stages of SSHDOM are the same as those of SHDOM. These include the computation of the optical properties of the medium, the delta-M scaling method, the TMS correction, and the computation of the radiance at a specified point and direction by means of the source integration method.
6. Comparing Algorithms 1 and 2, we see that SSHDOM involves some additional steps (written with italic fonts). These are (i) the computation of the DOF source functions $\widehat{J}_{0uv}(z_n, \widehat{\mathbf{\Omega}}_{ij}; \widehat{I}^{(k-1)})$ inside the Picard loop, and (ii) the computation of the initial SHF radiances $\widehat{I}^{(0)}_{lm;uv}(z_n)$, as well as of the SH source functions $J_{lm}(\mathbf{r}_n; \cdot)$ outside this loop. Therefore, we expect that SSHDOM is more time consuming than SHDOM.

4. Numerical analysis

The goal of our numerical simulations is the analyze the accuracy of SSHDOM using SHDOM as a reference. For simplicity, we consider a two-dimensional geometry, i.e., $I = I(x, z; \widehat{\mathbf{\Omega}})$, because this setting is sufficient to verify the correctness of the method.

The domain of analysis is a rectangle with length L and height H. The Gaussian beam, propagating in the xz-plane ($\varphi_0 = 0°$), is given by (cf. Eqs. (4) and (5))

$$\begin{aligned}I_0(x, z) &= \exp\Big\{-\Big[\frac{x - x_0(z)}{s_{\mathrm{x}}}\Big]^2\Big\}\mathrm{e}^{-\tau_0(x,z)}, \\ x_0(z) &= \frac{L}{2} + (H - z)\tan(\pi - \theta_0),\end{aligned}$$

where the incident zenith angle is chosen as $\theta_0 = 150°$.

The number of points for computing the discrete Fourier transform along the x-axis is $N = 2U = 128$ and the grid spacing in the spatial domain is $\Delta l = 0.1\,\mathrm{km}$. We introduce the basic length

$$s_0 = \frac{\kappa\Delta l}{\pi}$$

where κ is a parameter, e.g., $\kappa = 30$, in terms of which, the standard deviations of the Gaussian beam profile $s_{\rm x}$ and the extinction fields $(s_{\rm extx}, s_{\rm extz})$ will be defined. Note that in Ref. [2], s_0 expressed as

$$s_0 = \frac{\kappa \Delta l}{\pi} = \frac{2\kappa}{N\Delta k} = \frac{\kappa}{U\Delta k} = \frac{\kappa}{K},$$

where $\Delta k = 2\pi/(N\Delta l)$ is the grid spacing in the wavenumber domain and $K = U\Delta k$ the half-length of the wavenumber interval, was identified with the beam waist radius of the Gaussian beam.

Some geometrical and optical parameters are chosen as follows.

1. Along the x-axis, the number of grid points is $N_{\rm x} = 129$ (thus, $N_{\rm x} = N + 1$), the grid spacing is $\Delta x = \Delta l = 0.1\,\text{km}$, and the length of the domain of analysis is $L = (N_{\rm x} - 1)\Delta x = 12.8\,\text{km}$. Along the z-axis, the number of grid points is $N_z = 21$, the grid spacing is $\Delta z = 0.1\,\text{km}$, and the height of the domain of analysis is $H = (N_{\rm z} - 1)\Delta z = 2\,\text{km}$.
2. The number of discrete ordinates is $(N_\mu = 48) \times (N_\varphi = 2N_\mu = 96)$, and the spherical harmonics truncation indices are $L = N_\mu - 1$ and $M = N_\varphi/2 - 1$.
3. The boundary surface is a Lambertian reflecting surface with a constant surface albedo $A = 0.2$.

The following test problems are considered in our analysis.

1. A Gaussian extinction field

$$\sigma_{\rm ext}(x, z) = 0.01 + 4\exp\Big[-\frac{\big(x - L/2\big)^2}{2s_{\rm extx}^2} - \frac{\big(z - H/2\big)^2}{2s_{\rm extz}^2}\Big]$$

   with $s_{\rm extx} = 4s_0$ and $s_{\rm extz} = 8s_0$. The single scattering albedo is $\omega = 0.9$, and a Henyey–Greenstein phase function with the asymmetry parameter $g = 0.6$ is considered.
2. A cloud described by a bounded cascade model of order 7 with a variance of 0.3 and a variance reduction factor of 0.8. The cloud is homogeneous in the vertical direction, while the cloud extinction field along the horizontal direction is

$$\sigma_{\rm ext}^{\rm cloud}(x) = 4 f_{\rm BC}(x)\exp\Big[-\frac{\big(x - L/2\big)^2}{2s_{\rm extx}^2}\Big],$$

   where $f_{\rm BC}(x)$ is the indicator function of the bounded cascade model, and $s_{\rm extx} = 10s_0$. The cloud bottom and top heights are $H_{\rm bot}^{\rm cloud} = 1.4\,\text{km}$ and $H_{\rm top}^{\rm cloud} = 1.8\,\text{km}$, respectively. The cloud is a cumulus polluted cloud with a modified Gamma size distribution

$$p(a) \propto a^\gamma \exp\Big[-\frac{\alpha}{\gamma}\Big(\frac{a}{a_{\rm mod}}\Big)^\gamma\Big]$$

   and a droplet size range between 0.02 and 50.0 μm. The cloud droplet scattering is computed with Mie theory at a wavelength of 330 nm. The parameters of the size distribution are $a_{\rm mod} = 3.53\,\mu\text{m}$, $\alpha = 8$, and $\gamma = 2.15$, in which case, the total numbers of expansion coefficients of the phase functions are 341. In addition to the cloud, molecular Rayleigh scattering is considered as background.
3. A broken cloud with a cloud fraction of about 0.7. The cloud extinction field, as well as, the geometrical and the microphysical parameters of the cloud are chosen as in the second test example.

In the simulations, the delta-M scaling method is not used, but the adaptive grid with a splitting accuracy of 10^{-3} is employed.

In Figs. 2–4, we illustrate the radiance at the top of the atmosphere in the viewing directions ($\theta = 0°, \varphi = 0°$) and ($\theta = 60°, \varphi = 0°$). The results correspond to the following values of the standard deviation of the Gaussian beam profile: $s_{\rm x} = s_0$, $s_{\rm x} = 2s_0$, $s_{\rm x} = 4s_0$, and $s_{\rm x} = 8s_0$. From the plots it is apparent that

1. SSHDOM and SHDOM yield almost identical results, and
2. when the standard deviation of the Gaussian beam profile increases, i.,e, the incident field get closer to a plane electromagnetic field, more details of the extinction field are reproduced by the top-of-atmosphere radiance.

Comparing the computational times, we found as expected, that SSHDOM is by a factor between 1.8 and 2.0 slower than SHDOM. Thus, although accurate, SSHDOM is less efficient than SHDOM.

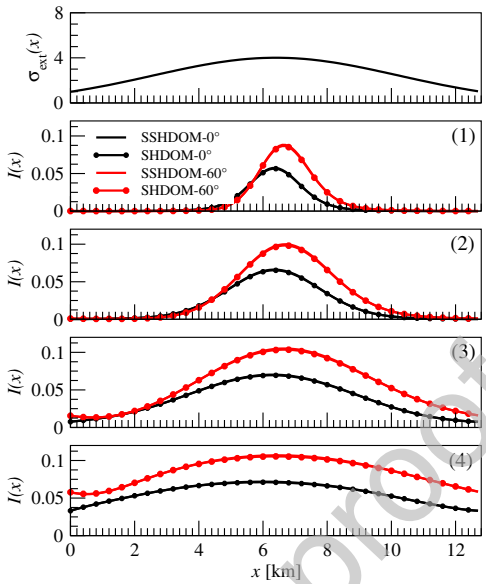

Figure 2: Radiance at the top of the atmosphere in the viewing directions $(\theta = 0°, \varphi = 0°)$ and $(\theta = 60°, \varphi = 0°)$ computed by SSHDOM and SHDOM. The results correspond to a Gaussian extinction field and to the following values of the standard deviation of the Gaussian beam profile: (1) $s_x = s_0$, (2) $s_x = 2s_0$, (3) $s_x = 4s_0$, and (4) $s_x = 8s_0$.

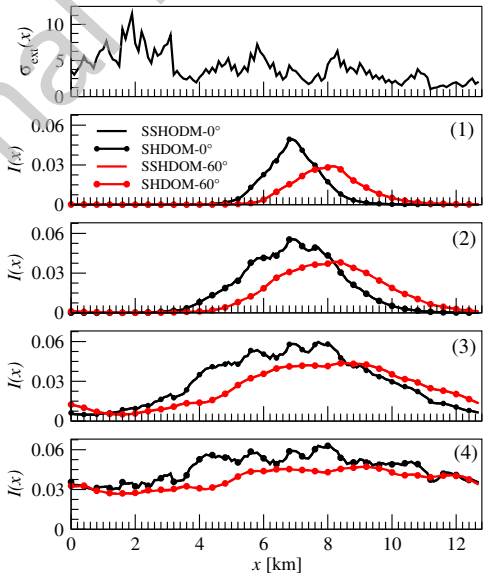

Figure 3: The same as in Fig. 2 but for a cloud described by a bounded cascade model.

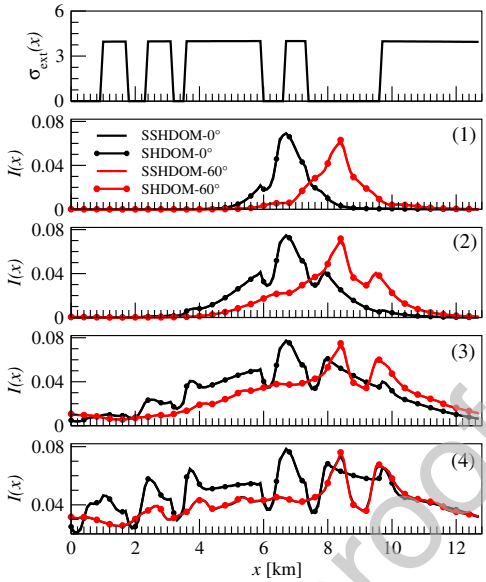

Figure 4: The same as in Fig. 2 but for a broken cloud.

5. Conclusions

The radiative transfer equation for an inhomogeneous three-dimensional medium illuminated by a Gaussian beam has been solved by using the spectral spherical harmonics discrete ordinate method. This approach

1. uses the Fourier expansion method to transform the three-dimensional radiative transfer into an one-dimensional equation in the spectral domain,
2. employs a spherical harmonic representation for the source function in the spectral domain to reduce memory use, and
3. integrates the spectral one-dimensional radiative transfer equation along discrete ordinates through a spatial grid.

The solution method is based on the Picard iteration.

The method is very similar to the spherical harmonics discrete ordinate method. What these methods have in common are

1. the transformation of the source function to discrete ordinates,
2. the integration of the radiative transfer equation along the discrete ordinates,
3. the transformation of the radiances to spherical harmonics,
4. the computation of the source function in the spherical harmonics space.

The difference is that in SHDOM, these steps are performed in the real space, while in SSHDOM, they are performed in the spectral or Fourier space. Because of this special feature, SSHDOM has to transform the radiance and source function between the real and Fourier spaces.

Due to the similarities of these methods, SSHDOM and SHDOM have been implemented in a common computer code. In this way, the two algorithms share the same pre- and post-processing steps which include the computation of the optical properties of the medium, the delta-M scaling method, the TMS correction method, and the computation of the output radiance by means of the source integration method. Although accurate, SSHDOM is less efficient than SHDOM. Therefore, in the new implementation, SSHDOM should not be regarded as an substitute for SHDOM, but rather as a comparison method.

Although our discussion was focused on a Gaussian beam illumination, SSHDOM is also appropriate to model optical and surface properties that are horizontally discontinuous or with abrupt changes.

References

[1] Doicu A., Mishchenko M.I., and T Trautmann. Electromagnetic scattering by discrete random media illuminated by a Gaussian beam I: Derivation of the radiative transfer equation. *J Quant Spectrosc Radiat Transfer*, 2020. Submitted.

[2] Doicu A., Mishchenko M.I., and T Trautmann. Electromagnetic scattering by discrete random media illuminated by a Gaussian beam II: Solution of the radiative transfer equation. *J Quant Spectrosc Radiat Transfer*, 2020. Submitted.

[3] Takahisa Kobayashi. Reflected solar flux for horizontally inhomogeneous atmospheres. *Journal of the Atmospheric Sciences*, 48(22):2436–2447, November 1991.

[4] David J. Diner and John V. Martonchik. Atmospheric transfer of radiation above an inhomogeneous non-Lambertian reflective ground—II. Computational considerations and results. *Journal of Quantitative Spectroscopy and Radiative Transfer*, 32(4):279–304, October 1984.

[5] Graeme L. Stephens. Radiative transfer in spatially heterogeneous, two-dimensional, anisotropically scattering media. *Journal of Quantitative Spectroscopy and Radiative Transfer*, 36(1):51–67, July 1986.

[6] P. M. Gabriel, S-C. Tsay, and G. L. Stephens. A Fourier–Riccati Approach to Radiative Transfer. Part I: Foundations. *Journal of the Atmospheric Sciences*, 50(18):3125–3147, September 1993.

[7] K. Franklin Evans. The spherical harmonics discrete ordinate method for three-dimensional atmospheric radiative transfer. *Journal of the Atmospheric Sciences*, 55(3):429–446, February 1998.

[8] K. F. Evans. Spherical harmonic discrete ordinate method (shdom) for atmospheric radiative transfer. https://coloradolinux.com/shdom/.

[9] T. Nakajima and M. Tanaka. Algorithms for radiative intensity calculations in moderately thick atmospheres using a truncation approximation. *Journal of Quantitative Spectroscopy and Radiative Transfer*, 40(1):51–69, July 1988.

The authors declare that they have no known competing financial interests or personal relationships that could have appeared to influence the work reported in this paper.

1. Adrian Doicu: Conceptualization; Formal analysis; Methodology; Writing-original draft; Writing – review & editing.
2. Michael Mishchenko: Conceptualization; Formal analysis; Methodology; Writing-original draft.
3. Dmitry Efremenko: Conceptualization; Methodology; Software; Writing-original draft; Writing – review & editing.
4. Thomas Trautmann: Conceptualization; Methodology; Supervision; Writing-original draft; Writing – review & editing.